Available online at www.sciencedirect.com

ScienceDirect

Procedia Engineering 00 (2016) 000–000

Procedia Engineering

www.elsevier.com/locate/procedia

1st International Conference on the Material Point Method, MPM 2017

Modeling dike failure using the material point method

Mario Martinelli[a,*], Alexander Rohe[a], Kenichi Soga[b]

[a]*Deltares, Delft, The Netherlands*
[b]*Engineering Department, University of Cambridge, UK*

Abstract

In this study, the material point method (MPM) is used to simulate and analyze the onset and evolution of the failure of a sand dike due to seepage flow. To that purpose, a MPM formulation in conjunction with an elastic-perfectly plastic soil model with Mohr-Coulomb failure criterion is used. For comparison, the onset of failure is also simulated with the standard finite element method. The results show that the double-point MPM formulation can satisfactorily model the essential features of the failure mechanism of the dike.

Peer-review under responsibility of the organizing committee of the 1 st International Conference on the Material Point Method.

Keywords: material point method; failure; fluidisation.

1. Introduction

The safety of dams, dikes and embankments is an important issue in many areas worldwide. In particular, in the Netherlands the problem has a great impact because three major European rivers (the Rhine, Meuse, and Scheldt) flow through the country protected by over 18000 km of dikes. The failure of a dike may compromise the safety of the country, since approximately 27 percent of the Netherlands is below sea level and in this area over 60 percent of the country's population (almost 16 million people) lives.

The failure of a dike can be caused by several mechanisms, e.g. macro-stability, overtopping, heave, piping, erosion (internal and external) which can be studied by using numerical or analytical methods. Some of these methods are mainly focused to identifying the conditions which lead to the onset of failure. However, nowadays the interest is extended to quantify the risks related to each failure mechanism, and for this reason methods that can fully

* Corresponding author.
E-mail address: mario.martinelli@deltares.nl

Peer-review under responsibility of the organizing committee of the 1 st International Conference on the Material Point Method.

describe the entire failure process from the beginning, where the displacements are small, to the very end after extremely large deformation are foremost important.

This paper describes the failure of a sand dike induced by seepage flow. This is a soil-liquid interaction problem which includes large deformation of soil, possibly together with fluidization and sedimentation of sand. Fluidization and sedimentation occur in the contact zone between soil and free surface water, where the conventional concepts of soil mechanics, based on the existence of a soil skeleton, do not longer apply and there is a transition zone between free surface water and solid skeleton. Such processes may occur in case of erosion of a dike induced by water flow, and the prediction of the final configuration is strongly related to the ability to correctly simulate both the failure mechanism together with fluidization-sedimentation processes.

Hence, the simulation of the entire process cannot be carried out using small-deformation analysis methods. The use of a large deformation analysis approach such as the recent advances of material point method (MPM) that can take into account the interaction of soil and water is rather more appropriate.

The original formulation of MPM was developed by Harlow (1964) [1] for fluid mechanics and then applied to solid mechanics [2] and dry granular materials [3, 4, 5]. Later, the method was extended to handle saturated soils [6] with a numerical approach which uses the velocity of both solid and liquid constituent as the primary unknowns. This formulation was applied to several small and large deformation problems and is able to capture the physical response of saturated soil under dynamic loading. However, only one set of material points is used for both the solid and the liquid phase; therefore groundwater flow and the transition between free surface water and groundwater cannot be captured as well as fluid-like behavior of the soil, which is typical for fluidization and sedimentation problems. Recently, a formulation with two sets of material points (so-called *double-point* formulation) was proposed [7, 8, 9, 10] to overcome such difficulties. Extensions to the original *double-point* formulation were first presented in [11] and then extended in [12].

Since the sand dike failure due to seepage flow is not only a soil-liquid interaction problem which includes large deformation of soil but also involves fluidization and sedimentation of sand, the *double-point* formulation [12] is used in the current study. Concepts of the *double-point* formulation are summarized in the following section.

2. Concepts of the double-point MPM

The motion of both solid and liquid material points is described by the system of momentum balance equations, using the velocity fields $\boldsymbol{v}_S$ and $\boldsymbol{v}_L$ for solid and liquid constituents, respectively:

$$\nabla \cdot \boldsymbol{\sigma}'_S + (1-n)\nabla \cdot \boldsymbol{\sigma}_L + \bar{\rho}_S \boldsymbol{g} + \boldsymbol{f}_d = \bar{\rho}_S \frac{D^S \boldsymbol{v}_S}{Dt} \tag{1}$$

$$n(\nabla \cdot \boldsymbol{\sigma}_L) + \bar{\rho}_L \boldsymbol{g} - \boldsymbol{f}_d = \bar{\rho}_L \frac{D^L \boldsymbol{v}_L}{Dt} \tag{2}$$

The terms $\bar{\rho}_S$ and $\bar{\rho}_L$ are respectively the partial densities of the solid and liquid, computed as the ratio of the mass of each constituent with respect to the reference volume; n is the soil porosity, and $\boldsymbol{\sigma}'_S$ and $\boldsymbol{\sigma}_L$ are respectively the effective stress tensor for solid and the stress tensor for liquid. $\boldsymbol{g}$ is the gravity vector. $D^\alpha \boldsymbol{v}_\alpha / Dt$ indicates the material time derivative of $\boldsymbol{v}_\alpha$ with respect to the movement of the constituent α.

In equations (1) and (2), $\boldsymbol{f}_d$ is the drag force vector exerted by the liquid on the solid part, and the Forchheimer [12] equation is used to compute it as:

$$\boldsymbol{f}_d = n^2 \frac{\mu}{\kappa}(\boldsymbol{v}_L - \boldsymbol{v}_S) + \frac{F}{\sqrt{\kappa}} n^3 \rho_L \,|\, \boldsymbol{v}_L - \boldsymbol{v}_S \,|\, (\boldsymbol{v}_L - \boldsymbol{v}_S) \tag{3}$$

where μ is the dynamic viscosity of liquid and κ is the soil intrinsic permeability. The first term in equation (3) is commonly named the Darcy term whereas the second term describes the additional drop of the hydraulic head

observed at high flow velocities, which is common in soils with large porosity. The Kozeny-Carman formula [13] is used to update the soil intrinsic permeability as follows

$$\kappa = \frac{D_p^2}{A}\frac{n^3}{(1-n)^2} \tag{4}$$

where D_p is the grain size diameter and the coefficient F is computed as:

$$F = \frac{B}{\sqrt{A}n^{3/2}} \tag{5}$$

where A and B are constant values set respectively to 150 and 1.75 [8].

The fluidization and sedimentation process can be described in this formulation by defining first the behavior of fluidized and non-fluidized mixtures. The soil porosity n is the parameter used to distinguish between the two aforementioned states. In low-porosity mixtures, the grains of the solid skeleton are in contact and the behavior is described by constitutive models developed for granular materials (*solid-like* response). Conversely, in high-porosity mixtures the grains are not in contact and float together with the liquid phase. In this case, the effective stresses are equal to zero and the response of the mixture is described by the Navier-Stokes equation (*liquid-like* response). The two aforementioned states are distinguished through the maximum porosity n_{max}, which is the maximum value of the porosity for a given soil in its loosest state. In case of *solid-like* response, the effective stress rate in solid MPs is calculated using the soil constitutive law. In case of *liquid-like* response, the effective stress in solid MPs is set to zero. The fluidization occurs only if the grains are significantly separated, so that the porosity is larger than n_{max}. In the reverse process, i.e. the sedimentation of a fluidized mixture, the porosity decreases due to the fact that the solid grains get closer to each other. However, the effective stresses recur only if the porosity is smaller than n_{max}, i.e. the grains are close enough to be in contact.

3. The failure of a dike due to seepage flow

The *double-point* MPM formulation is used to model the failure of a dike due to seepage flow. The problem refers to a small-scale dike and the geometry is shown in Fig. 1. The height of the dike is 1 m, the base is 4.2 m and the slope angle is approximately 27 degrees. The dike is made of homogeneous monogranular sand (D_p = 2 mm) with absence of fines, and is built on a stiff and impermeable rock layer. The height of the upstream reservoir is assumed to be 0.8 m at the beginning of the simulation. The hydraulic head is initialized as shown in the figure.

Only the downstream side of the dike is studied, considering the domain A-B-C, and the hydraulic head is assumed equal to the reservoir on the line A-B (i.e. no head loss in the upstream part of the dike with respect to the line A-B).

A linear elastic perfectly plastic constitutive model with a Mohr-Coulomb failure criterion is used for the solid skeleton and a Newtonian compressible constitutive model is used for the liquid. The parameters for both constitutive models are listed in Table 1.

The Anura3D [17] code is used for the simulations and it has only tetrahedral elements. Plane-strain conditions are assumed in the simulation by considering only one row of tridimensional elements. The computational mesh shown in Fig. 2 consists of 16695 4-node tetrahedral elements.

At the beginning of the calculation, 8 material points (MPs) per element (4 liquid and 4 solid MPs) are assigned to the soil domain and 10 MPs are assigned to the free water. The upstream and downstream water reservoirs have a width respectively 2 m and 1 m. No inflow or outflow boundary condition can be specified in the current version of Anura3D [17], i.e. material points cannot be added or removed during the simulation in order to keep the upstream water level constant. For this reason, the water level changes in the reservoirs during the simulation as the liquid material points move from the upstream to the downstream side.

At all boundaries the displacements are constrained in normal direction and free in the longitudinal one. The rock surface is modeled as fully rough, so that the solid displacements are fully constrained in horizontal direction. The horizontal displacements are also constrained for the solid material points along the cross section A-B.

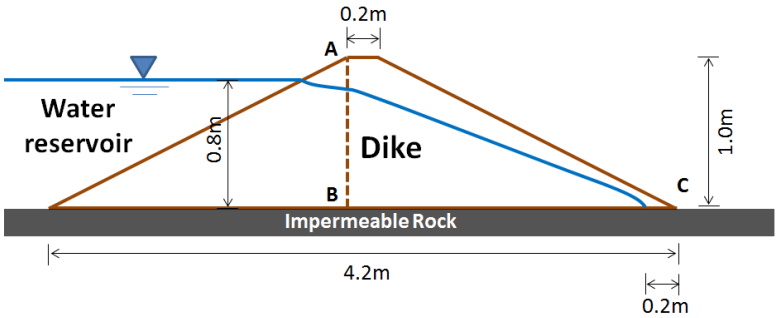

Fig. 1. Geometry of the problem.

Table 1. Parameters of the constitutive models.

Material parameter	*Symbol*	*Value*	*Unit*
Density of grains	ρ_S	2700	kg/m^3
Young modulus	E	1000	kPa
Poisson ratio	ν	0.15	-
Initial porosity	n	0.4	-
Maximum porosity	n_{max}	0.5	-
Grain diameter	D_p	2	mm
Friction angle	φ	35	degrees
Dilatancy angle	ψ	5	degrees
Cohesion	c	0	kPa
Water density	ρ_L	1000	kg/m^3
Water bulk modulus	K_L	20000	kPa
Water viscosity	μ	8.905 10^{-7}	kPa s

The initial stress in the soil and free water is calculated during an initial phase by linearly increasing the gravity acceleration from 0 to 9.81 m/s^2, so that the system can gradually update the stress distribution in equilibrium with the external forces and the boundary conditions. During this phase, the horizontal displacements of the water are constrained; this boundary condition is removed during the subsequent phases.

The soil permeability is calculated according to Kozeny-Carman formula [13] using the updated porosity, resulting in k = 5.3 cm/s at the beginning of the simulation. Since Equations (1) and (2) are solved with an explicit time integration scheme, the bulk modulus of the water is reduced by a factor of 20 in order to reduce the computational time but still large enough compared to the bulk modulus of the solid skeleton. The results are shown only over a limited part of the domain labeled as “area of interest” (AOI) as shown in Fig. 2.

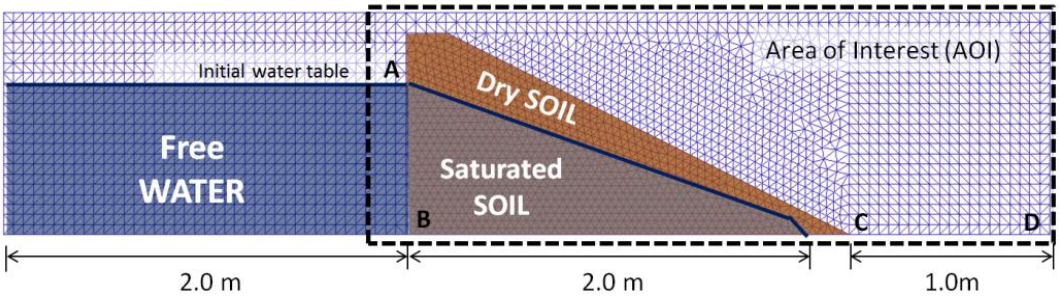

Fig. 2. Discretised domain of the simulated problem.

3.1. MPM results

Fig. 3 shows the soil porosity at the location of the solid material points for t = 6, 8, 14 and 23 seconds, together with the position of the liquid material points. The porosity can vary approximately from 0.4 to 1.0 but the legend has a narrower limit to focus on the range below the maximum porosity ($n < n_{max}$).

The initial porosity is set to 0.4. As soon as the simulation starts, pore pressures at the toe of the dike increase and the drag forces exerted by the water flow tend to move the solid material points to the right of the domain into the empty reservoir. Plastic shear strains are induced into the soil and, due to the positive dilatancy angle, the porosity increases accordingly. Initially (t=6s) the porosity increases only at the toe of the dike whereas, as the simulation proceeds (t=8s), the change in porosity propagates also along the shear plane. At the toe of the dike, the porosity of the soil increases until it exceeds the maximum porosity and fluidizes.

As the time passes (t=14s) the extension of the fluidized zone progressively increases, moving backwards from the toe of the dike towards the crest, and the fluidized material located at the toe of the dike is moved into the downstream reservoir due to the water flow. Such a movement is very slow in time since the bottom boundary for the soil is modeled as perfectly rough. Such a boundary condition is rather an extreme case and can represent the condition offered by a rough and irregular rock surface with many vertical fractures.

Large increase in porosity is also observed along the failure surface (t=23s), where some solid material points have a *fluid-like* behavior. This evidence is not realistic and it is associated to the extremely simplified constitutive model which has a constant dilatancy angle, independent of the plastic strains. Therefore, along the failure surface where most of the shear strains are concentrated, the response of the constitutive model produces a progressive increase in volume which leads the soil to overcome the range of *solid-like* behavior.

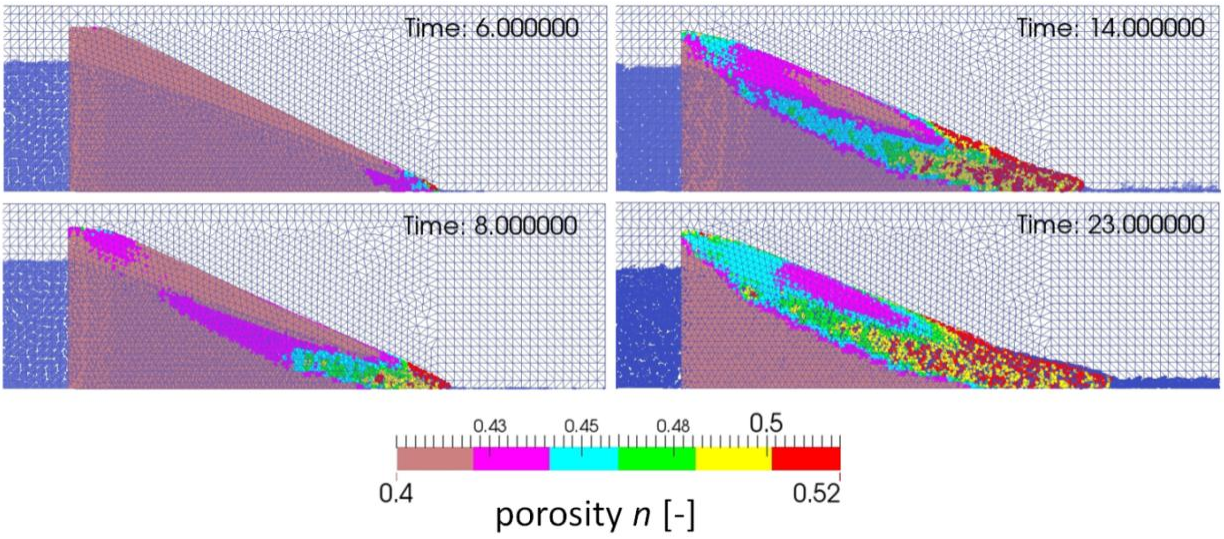

Fig. 3. Liquid material points and porosity of solid material points.

3.2. Modeling the onset of failure with FEM

For comparison, the problem is also simulated using the FE method with the commercial code PLAXIS 2D [16], where the small strain FE formulation is used to model the onset of failure. Figure 4 shows the computational mesh (1640 15-node triangular elements) together with the two materials defined for this problem, both modeled as soils. *Soil1* represents the dike where the seepage and most of the hydraulic losses take place. Conversely, *Soil2* is used on both sides of Soil1 to fictitiously simulate the reservoirs for the free-water.

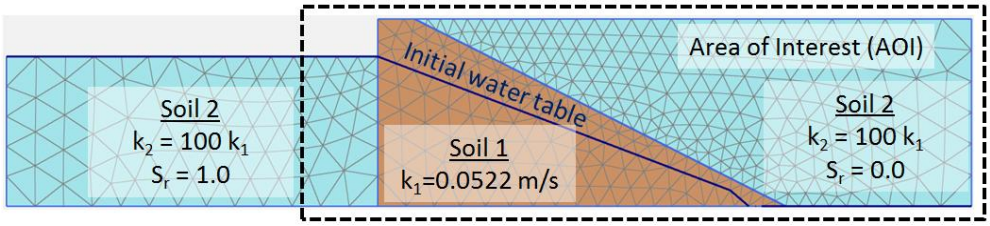

Figure 4: Computational mesh in PLAXIS 2D.

The soil parameters (for *Soil1*) are the same as those used in the MPM simulations. *Soil2* is modeled as linear elastic material and Table 2 shows the mechanical parameters. The Van Genuchten model is used in *Soil1* and *Soil2* to describe the transient water flow through the dike and the water reservoirs. The parameters of the Van Genuchten model are listed in Table 3, where g_a, g_n and g_l are fitting parameters: g_a is related to the air entry value of the soil, g_n is a function of the rate of water extraction from the soil as soon as the air entry value has been exceeded, and g_l affects the decrease of permeability with suction.

It is worth noticing that only the Darcy term is used in PLAXIS to calculate the soil-water viscous interaction (first term in equation 3). For this reason, an additional MPM analysis is performed using the Darcy law and the results are compared in Figure 5. The results are represented only in the "area of interest" (AOI), as shown in Figure 4.

Table 2: Parameters of the constitutive models of Soil-2.

Material parameter	*Symbol*	*Value*	*Unit*
Dry unit weight	γ_{dry}	0.01	kN/m^3
Saturated unit weight	γ_{sat}	10.01	kN/m^3
Young modulus	E	1	kPa
Poisson ratio	ν	0.45	-

Table 3: Parameters of the van Genuchten model.

Material parameter	*Symbol*	*Value*	*Unit*
Change of permeability	c_k	0.875	-
Residual saturation	S_{res}	0.05	-
Maximum saturation	S_{sat}	1	-
Fitting parameter	g_a	25	1/m
Fitting parameter	g_n	3	-
Fitting parameter	g_l	5	-
Fitting parameter	g_l	5	-

The FE results show the deviatoric strain contour together with the position of the water table for three time instants: 2, 6 and 14 seconds. As the analysis starts, the pore pressures at the toe of the dike increase and the soil strength decreases, so that strains are developing. Initially (t=2s) the deviatoric strains are concentrated at the toe of the dike whereas, as the time proceeds (t=5 and 14s), the shear strains are also propagated along the failure plane.

The failure mechanism described using FE analysis is the same as the one with the MPM. Indeed, initially the porosity increases (as a result of the positive dilatancy angle) at the toe of the slope and then such a volume change propagates along the failure surface. The dimension of the soil mass above the failure surface is the same in both simulations, and the position of the water table throughout the computational domain is approximately the same in both FE and MPM for each time instant.

It is worth noticing that the failure process shown in Figure 5 with the Darcy law is faster than the one presented in Fig. 3, which is computed with the Forchheimer law with Ergun coefficients. In case of Darcy law the complete failure surface is clearly identified after 6 seconds whereas for the Forchheimer law the same condition occurs only after 8s. Such a significant difference highlights the importance of using a more advanced expression to calculate the drag forces (e.g. Forchheimer equation) compared to the Darcy law in order to have an accurate description in time of the failure process.

Lastly, it is worth mentioning that the FE analysis cannot provide any additional information regarding the evolution of the failure process after the complete mobilization of the strength along the failure surface. Such information can be obtained when taking into account large deformations by updating the mesh (Updated-Lagrangian formulation). However, in this case, even the large deformation approach suffers from element distortion and cannot be used. Therefore, MPM seems to be a suitable approach for this purpose as it can simulate the problem from the beginning, where the displacements are small, towards the end after extremely large deformation.

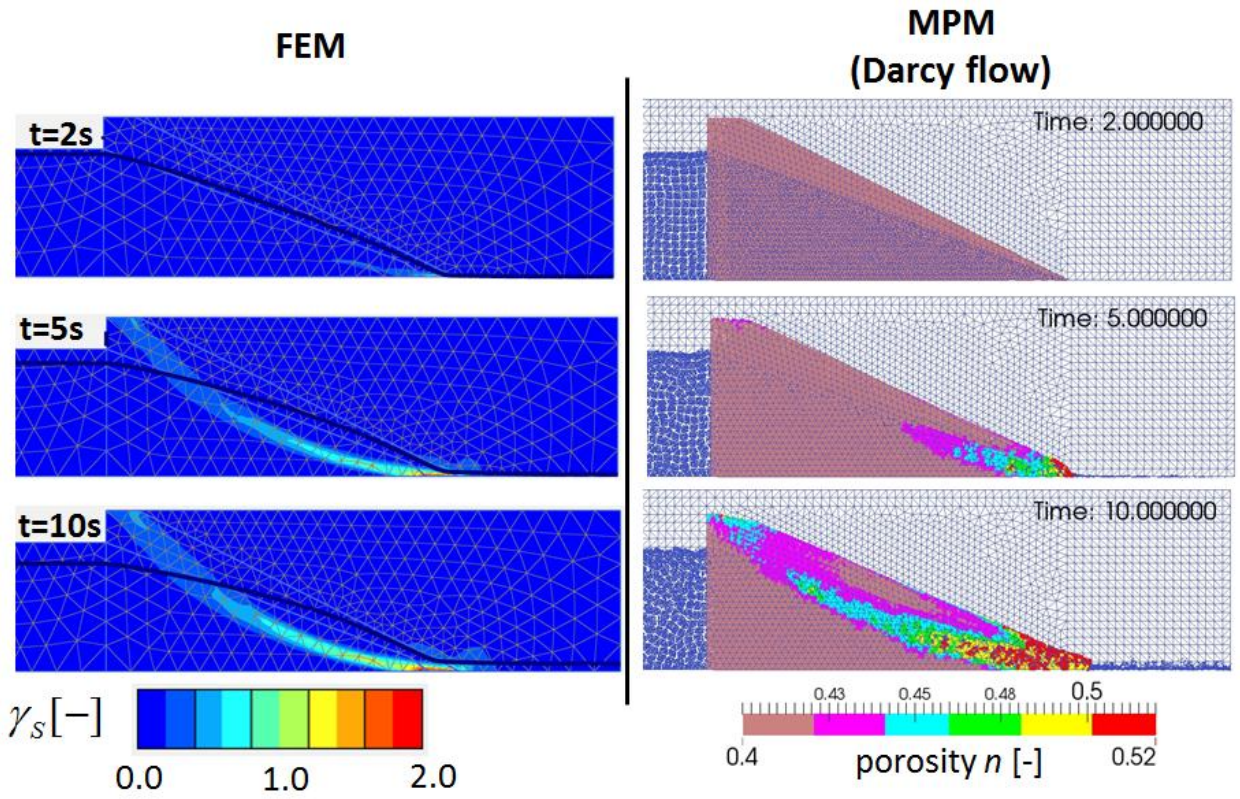

Figure 5: (left) Deviatoric strains obtained from FE simulations. (right) MPM results using Darcy law.

4. Conclusions

The onset and the progression of the sand dike failure due to seepage flow are successfully simulated in this study using the *double-point* MPM formulation using Anura3d [17]. It is shown that MPM can satisfactorily simulate the problem. The onset of failure is also simulated using the FEM to verify the MPM results; however, the small-strain FEM analysis cannot provide any additional information regarding the evolution of the slope failure, and even the large deformation FE approach cannot be implemented as it suffers from element distortion.

It is worth mentioning that the use of Mohr-Coulomb constitutive model is only a first attempt. However, in future analyses a more advanced critical state constitutive model is necessary for modeling more realistic soil behavior.

References

[1] Harlow F.H. The particle-in-cell computing method in fluid dynamics. Methods in Computational Physics., (1964) 3, pp 319-343.
[2] Sulsky D., Zhou S., Schreyer H.L. Application of a particle-in-cell method to solid mechanics. Computer Physics Communications. (1995),87, pp 236-252.
[3] Wieckowski Z. A particle-in-cell method in analysis of motion of a granular material in a silo. In: Computational Mechanics: New Trends and Applications, CIMNE, Barcelona. (1998)
[4] Wieckowski Z., Youn S.K., Yeon Y.H. A particle-in-cell solution to the silo discharging problem. Int. J. Numer. Meth. Engng., (1999), 45, pp 1203-1225.
[5] Wieckowski Z. Modelling of silo discharge and filling problems by the material point method. Task Quarterly, (2003), 4, pp 701-721.
[6] Jassim I., Stolle D., Vermeer P.A. Two-phase dynamic analysis by material point method. International Journal for Numerical and Analytical Methods in Geomechanics 37(15), 2502-2522, (2013). DOI:10.1002/nag.2146
[7] Bandara S., Soga K. Coupling of soil deformation and pore fluid flow using material point method. Computers and Geotechnics (2015) 63, 199-214. DOI:10.1016/j.compgeo.2014.09.009.
[8] Bandara S. Material Point Method to simulate large deformation problems in fluid-saturated granular medium. Ph.D. Thesis University of Cambridge (2013).
[9] Vermeer P.A., Wieckowski Z., Sittoni L., Beuth L. Modelling Soil-Fluid and Fluid-Soil Transitions with Applications to Tailings. In: Tailings and Mine Waste (2013) (November 3-6, 2013), Ban, Alberta, Canada, pp. 305-315.
[10] Więckowski Z. (2013). Enhancement of the Material Point Method for Fluid-Structure Interaction and Erosion. Report on EU-FP7 research project Geo Fluid PIEF-GA-2010-274335.
[11] Martinelli M. and Rohe A., 2015. Modelling fluidization and sedimentation using Material Point Method. 1st Pan-American Congress on Computational Mechanics - PANACM 2015. XI Argentine Congress on Computational Mechanics - MECOM 2015. S. Idelsohn, V. Sonzogni, A. Coutinho, M. Cruchaga, A. Lew & M. Cerrolaza (Eds)
[12] Martinelli M. (2016). Soil-water interaction with Material Point Method. Double-Point Formulation. Report on EU-FP7 research project MPM-Dredge PIAP-GA-2012-324522.
[13] Forchheimer, P., 1901. “Wasserbewegung durch Boden. Z Ver Deutsch Ing 45: 1782-1788.
[14] Bear J. Dynamics of fluids in porous media. New York: Elsevier (1972)
[15] Ergun, S. Fluid flow through packed columns. Chem. Engng Prog. (1952) 48, 89-94
[16] Plaxis2D – version 2016. www.plaxis.nl
[17] Anura3D - http://www.anura3d.com